Solvent Compatible Microfluidic Platforms for Pharmaceutical Solid Form Screening

Sachit Goyal,[ac] Aristotle E. Economou,[#a] Theodore Papadoupolos, [#a] Elizabeth M. Horstman,[a]

Geoff G.Z. Zhang,[b] Yuchuan Gong, *[b] and Paul J.A. Kenis*[a]

S1. Effect of harsh organic solvents on PDMS-COC based microfluidic platforms

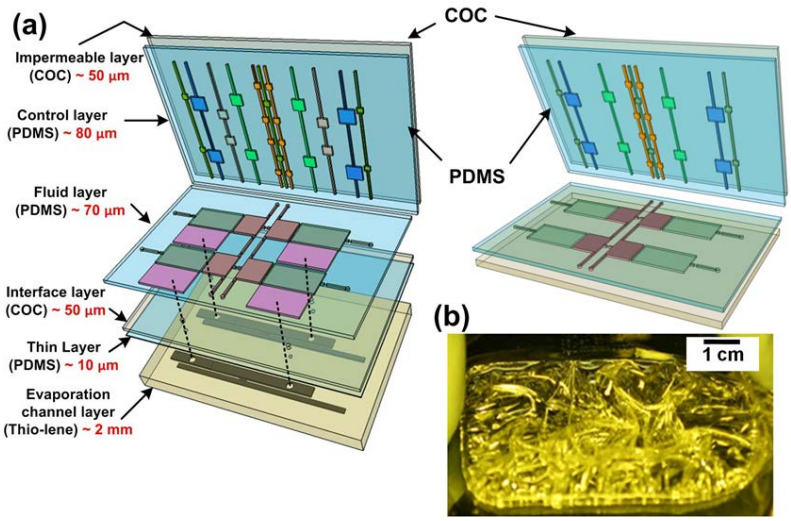

Figure S1 (a) Schematic of the diffusive mixing-based and solvent evaporation-based microfluidic platforms. (b) Swelling of PDMS on exposure to hexane solvent.

Materials and Methods

Chip Assembly

a. Four-layer assembly (FLA) fabrication: FLA is comprised of a SIFEL (Shin-Etsu Silicones of American Inc., Part A/B) control layer (CL) and fluid layer (FL), a polydimethylsiloxane (PDMS, General Electric RTV 615, Part A/B) adhesion layer, and a cyclic olefin copolymer (COC) (COC, 6013 grade, TOPAS^{TM} Advanced Polymers) backing layer (Figure 2a). Control layer and fluid layer were prepared by spin coating 1.5:1 A:B SIFEL and 1:1.5 A:B SIFEL, respectively, onto silicon waters patterned with a

negative photoresist SU-8 2050 (MicroChem) and cured at 100°C in a convective oven. A thin layer of 15:1 A: B PDMS was spun coated on the partially cured CL and cured at 110°C on a hot plate (Dataplate® 730 series, Barnstead Thermolyne). A 100 μm COC layer was irreversibly bonded onto the PDMS-CL assembly via plasma oxidation and further heated at 110°C for about 2 hours. The COC-PDMS-CL assembly was then carefully lifted off the CL master while the master was on the hot plate. Holes were drilled (Dremel 300 series drill with a 750 μm McMaster-Carr drill bit) at the inlets of the control lines. Subsequently, the COC-PDMS-CL assembly was manually aligned on the FL and the further cured at 120°C on a hot plate to prepare the monolithic FLA. Through holes were drilled at the inlets and outlets in the FL. The diffusive-mixing/ antisolvent addition based microfluidic platform was prepared by reversibly bonding the FLA onto a Teflon sheet or COC sheet depending on the solvent used to complete the assembly.

Next, a 3 mm thick SIFEL block with a thin layer of PDMS (for adhesion) was irreversibly bonded to the top of the FL, followed by punching of through holes into the thick layer. The block was prepared by spin coating (1300 RPM) and partial curing of a thin layer of PDMS (10:1 A:B, 65°C) on a Si wafer and simultaneously partially curing a thick block of SIFEL (100°C). Next, the partially cured SIFEL block and PDMS film were brought in contact and the system was fully cured in the oven at 100°C. The SIFEL block along with the thin PDMS film was then lifted off from the silicon wafer and bonded to the top of the FL by treatment via oxygen plasma.

b. Interfacial layer (IL) fabrication: A thin layer (40 μm) of PDMS (5:1 A/B) was spin coated at 1500 rpm on a blank silicon wafer pre-coated with a monolayer of tridecafluoro-1,1,2,2-tetrahydrooctyltrichlorosilane (Gelest). The thin layer of PDMS was then semi cured on a digital hot plate / stirrer (Dataplate® 730 series, Barnstead Thermolyne) at 80°C for approximately 5 minutes. A 50-100 μm thick Teflon FEP or AF (Dupont) sheet was reversibly sealed to the top of the PDMS layer and further heat cured at 110°C on the hot plate. The assembly was carefully observed for 5minutes and bubbles propagating between the layer were pushed out. A thin layer of SIFEL was spin coated on the Teflon placed on the silicon wafer and cured thermally at 110°C on a hot plate. The Teflon-SIFEL assembly was then lifted off from the PDMS layer and the SIFEL side of the assembly was covered with Scotch™ removable tape as shown in Figure 2b.

c. Evaporation layer (EL) fabrication: The EL was fabricated out of NOA–81 thiolene (Norland Products) as described in previous work with several modifications.[52, 54, 70] Thiolene allows for replication of sub-micron features, as well as features with large aspect ratios due to its higher elastic modulus compared to PDMS. Thiolene is optically translucent enabling imaging via optical microscopy.[52] Figure 2c provides an overview of the fabrication steps employed to create the EL. Positive photoresist (SPR 220-7, Rohm and Haas Electronic Materials) was patterned on a 4" silicon wafer. Microchannels, 50 or 100 μm tall, were etched in the wafer by deep reactive ion etching (DRIE, PlasmaTherm ICP-DRIE etching system) for 30 minutes or 1 hour. Next, the photoresist was washed away with acetone and the residual impurities on the wafer were removed by oxygen plasma (RIE, March Jupiter III). The etch depth was confirmed by profilometry (KLA Alphastep IQ). The etched wafer was coated with a monolayer of silane. Then a PDMS replica was prepared by pouring 5:1 A/B PDMS onto the

etched silicon wafer and cured by heating in a convection oven (Thermo Scientific) at 65°C for 1-2 hours. The resulting PDMS mold was lifted off the etched silicon wafer and a 3" x 2" PDMS window frame (10:1 A/B PDMS), ~2 mm in height, was reversibly sealed on the side of the PDMS mold with embossed features. The resulting structure will allow for replication of the embossed features in thiolene. The inner dimensions of the PDMS frame defined the outer dimensions (overall size) of the thiolene replica. Liquid thiolene was pipetted into the PDMS mold while avoiding the formation of bubbles, until it was completely filled to the edge of the frame. A microscope slide was placed on top of the PDMS mold to remove any excess thiolene and to provide rigidity. The liquid thiolene was then cured by UV exposure (OAI flood exposure system; intensity 10.8 mW/cm^2) for 6-10 minutes on one side, and then flipped and exposed again for another 6-10 minutes.[71] The glass slide bonds to thiolene upon curing and ensures that the formed, patterned thiolene layer remains flat and rigid. The thiolene layer, still bonded to the glass slide, was then removed from the PDMS mold.

d. Alignment and final assembly of all layers. First, the IL was placed on the EL so the location of through-holes needed to connect the evaporation chambers in the FLA and the corresponding evaporation channels in EL could be marked. Then, after removing the EL, holes were drilled in the marked locations of the IL (Dremel 300 series, 100 μm McMaster-Carr drill bit). Next, the IL was manually aligned and reversibly sealed to the EL. Finally, the FLA was manually aligned and reversible sealed to the IL-EL assembly such that the holes in the evaporation chambers in the FL were aligned with the corresponding evaporation channels. These alignment steps were performed under an optical microscope (Leica MZ6) for accuracy. The alignment steps complete the fabrication and assembly of the complete chip for cocrystal

screening via evaporative crystallization as shown in Figure 2d. Figure 2 shows detailed views of the assembly of different layers of the chip for evaporation driven crystallization experiment.

Filling and Mixing of the Solutions in the Microfluidic Chips: All solutions were introduced into the chambers within the chip following a similar procedure as described previously for the 48-well microfluidic platform for cocrystal screening of APIs.[48] Each inlet corresponding to an API or CCF/antisolvent solution was connected via tubing (30 AWG thin-walled PTFE, Cole Parmer) to a 0.65 mL micro-centrifuge vial (VWR International) filled with an API or a CCF/ antisolvent solution. To avoid solvent evaporation from the centrifuge vials, the tubing was inserted through a 1-mm hole drilled into the cap of the vial. The solutions were introduced to the chambers on-chip upon actuation of the appropriate set of valves (*vide infra*) while simultaneously applying gentle suction at corresponding fluidic outlets. Once filled, the API and CCF/antisolvent solutions were allowed to mix for about an hour. After the solutions were fully mixed, peripheral connections such as tubing for filling were disconnected, the inlets and outlets of the chip were sealed. All fluidic inlets and outlets were covered with Crystal Clear Tape (Hampton HR4-511) to inhibit solvent loss. In case of the solvent evaporation chip, after the mixing of the API and CCF solutions, the valves that allow for evaporation were actuated to allow solvent to escape through the evaporation channels and thereby initiate the evaporation driven crystallization experiments.

Visualization of the Crystallization Experiments: The wells were periodically monitored for appearance and growth of solids throughout the on-chip crystallization experiment using an automated imaging system comprised of an optical microscope (Leica Z16 APO) equipped with an auto-zoom lens (Leica 10447176), a digital camera (Leica DFC280), and a motorized X-Y stage (Semprex KL66) controlled by Image Pro Plus 7.1 software (Media Cybernetics). Images

of each well were acquired every 5-20 minutes depending on the total length of the experiment by moving the automated motorized stage in a sequential manner from well to well. At the end of each experiment, after removing the highly birefringent EL, dark field images of each well were acquired using crossed polarizers to confirm the crystalline nature of the resulting solid forms.

Estimation of Solvent Evaporation Rates: The moving solvent interface in each microfluidic well was recorded at designated time points using the images captured via time-lapse optical microscopy and analyzed ("freehand selection" tool in ImageJ 1.46). The area and hence the volume (as the height of each well remains constant) occupied by the solution in each well was determined as a function of time. The rates of solvent evaporation were represented by the change in the volume fraction of the residual solution in each well.

Solid Form Analysis: The glass vials (off-chip) were examined under a microscope to determine the crystalline nature of the solids collected in the experiments. To analyze the solids formed on-chip, the thiolene layer was peeled off the FLA–IL assembly after the completion of on-chip crystallization experiments (after 2 to 50 hours). The crystalline nature of the solids in the FLA-IL assembly was verified using a stereomicroscope (Leica MZ12.5) equipped with a digital camera (Leica DFC295) under bright field as well as dark field using crossed polarizers (birefringence analysis).

The identity of each of the crystalline solid forms of carbamazepine and theophylline was verified by a Raman spectrometer equipped with a 785 nm excitation source (Renishaw NIR 100 mW diode laser) and connected to an upright microscope (Leica DM2500M). The microfluidic chip was placed in the sample holder and individual wells were centered in the bright field mode using 5x magnification (Leica 506302 objective, 5x/0.12NA), followed by use of higher

magnifications such as 20x (Leica 566066 objective, 20x/0.4NA) and/or 50x (Leica 566027 objective, 50x/0.75NA). The laser was then switched on and set at 10% laser power and the Raman spectra of individual crystals were collected in the range of 1050-1800 cm^{-1} for cocrystals and in the range of 600-1700 cm^{-1} for polymorphs by focusing the laser beam to a spot size of ~5 μm at 50x magnification with a long working distance objective (Leica 566036 objective, 50x/0.5NA) in the dark field mode.

The crystalline solids obtained off-chip were transferred onto a gold-coated glass slide for Raman analysis. Raman spectra of the solids were collected at 20x magnification and compared with those reported.[37, 73] Gold coated glass slides were prepared by coating pre-cleaned microscope slides (Fischer Scientific 12-550-A3) with a 20-nm layer of chromium for adhesion, followed by deposition of a 200-nm layer of gold using an E-beam evaporation system (Temescal six pocket E-Beam Evaporation System). Data collection was carried out at a spectral resolution of ~0.5 cm^{-1} at 1800 gratings/mm, with the exposure time set to 40s, and each spectrum was averaged over two accumulations.

Design of evaporation channels:

Most of the pharmaceutically acceptable CCFs that are most commonly used in early stage solid form screening, are small molecules and have high solubility in alcohol and water. Hence, high concentrations of the SF solutions can be introduced in the SF chambers on-chip. Therefore, the size of the CCF chamber is designed to be half the size of the PC chamber, which allows the CCF and PC to be mixed at equimolar ratio. In practice, PC and CCF solutions are frequently prepared in organic solvents and water, respectively. The smaller size of the CCF

chamber compared to the PC chamber reduces the chance of precipitation of PC upon mixing with aqueous solutions of CCF due to antisolvent effects.

The solutions of PC and CCF are mixed on-chip by diffusion. The time required to achieve complete mixing depends on the diffusivity of each component as well as the dimension of the chambers. The distance that a component travels by diffusion within a time *t* can be estimated using Fick's law, $l = 2(Dt)^{½}$. The combined length of the SF and the PC chambers was approximately 2.7 mm. The diffusivity *D* of the molecules used here is on the order of 10^{-9} m^2/s. Therefore, the solutions of PC and CCF will be completely mixed by diffusion in approximately one hour after the onset of mixing.

A third chamber, an evaporation chamber, was added to the fluid layer adjacent to each PC chamber. The evaporation chamber was connected to the PC chamber (containing the mixed PC/CCF solutions) through a control valve. The evaporation chamber was further connected to the atmosphere via evaporation channels in the EL, through which the solvent vapor can diffuse to the outside environment. The rate of solvent evaporation is determined by the dimensions of the evaporation channels. The rate of solvent evaporation is determined by the dimensions of the evaporation channels. The rate of solvent evaporation can be expressed by the following equation[28-30]:

$$J = \frac{DM}{RT}\Delta P\frac{A_C}{L} \quad \text{Or} \quad J = K\frac{A_c}{L} \qquad (1)$$

where

- J is the volumetric flow rate of solvent evaporating out of the chamber
- ΔP is the difference between the partial pressure of the solvent mixture in the evaporation chamber and that of the ambient, the atmosphere outside the chip
- D is the diffusivity of solvent vapor in air
- M is the molecular weight of the solvent mixture

R is the gas constant
T is the absolute temperature
A_c is the cross-sectional area of the evaporation channel
L is the length of the evaporation channel.

The solvent evaporation channels were redesigned taking into consideration that the microfluidic platform reported possess enhanced solvent resistance. **Table S1** shows a comparison chart of evaporation coefficient (K) of different solvents compared to water. Compared to water, the K value ranges from 1 to 30 with some exceptions, so the evaporation channels were designed for K values = 15 and 30. **Table S2** shows the dimensions of the evaporation channels corresponding to different solvent evaporation rates (computed analytically).

The evaporation rate of the solvent selected in the experiment is proportional to the difference in partial pressure, diffusivity of the solvent, and molecular weight of the solvent. The difference between the partial pressure of the solvent in the evaporation chamber and that of the ambient serves as the driving force for the evaporation of the solvent. The partial pressure of the solvent of the ambient remains constant, *i.e.* zero for the organic solvent, and equal to the relative humidity for water (assuming it does not change during the experiment). The concentration of the solute increases as the solvent is removed via evaporation. Thus, the partial pressure of the solvent in the evaporation chamber decreases with time. However, the change in the partial pressure of the solvent in the chamber can be ignored in cases where precipitation occurs before the solution becomes too concentrated. Therefore, we can consider that the driving force for solvent evaporation remains constant during the experiment.[17]

When a particular solvent is selected for the experiment, the evaporation rate can be controlled by the dimension of the micro-channels, as previously reported for PDMS and polypropylene platforms for droplet based crystallization.[16] Equation (1) suggests that the evaporation rate

increases if the evaporation chamber is connected to a shorter evaporation channel having a large cross-sectional area. The evaporation channels in the EL were designed such that the solvent in the 6 wells in the same row in a 4 x 6 microfluidic array chip evaporated at the same rate, while each row results in solvent evaporation at a unique rate. In addition to solvent evaporation through the evaporation channels, solvent loss can also occur due to solvent absorption by the chip materials, followed by evaporation of solvent to the outside of the chip. As a control experiment, we always filled six wells in one of the four rows in the microfluidic chip without connecting them to an evaporation channel. This allowed us to determine the rate of solvent loss due to absorption.

The rate of solvent loss in the microfluidic chips can be represented by the volume fraction of residual solvents in the chambers as a function time. Pure methanol escaped from the control wells in the PDMS chip at a rate of 4 nL/hr and from the wells in the other three rows at a rate of 16, 10, and 7 nL/hr, respectively. Thus, the rates of evaporation of methanol from the wells in the three rows connected to evaporation channels, adjusted for the control, are 12, 6, and 3 nL/hr. These experimentally determined rates are slightly smaller than the expected rates, calculated using equation 1, *i.e.*, 15, 7.5, and 3.75 nL/hr, respectively (K'=6 design).

Table S1. Solvent evaporation rate factor (K) for different solvents

	K	$K_{Solvent/Water}$ (K')
Water	0.004	1
Ethanol	0.024	5.599
Methanol	0.045	10.257
Isopropanol	0.013	2.951
Isobutyl alcohol	0.004	1.023
n-hexane	0.064	14.781
n-heptane	0.021	4.856
pentane	2.648	608.452
acetonitrile	0.032	7.455

DMF (Dimethyl Formamide)	0.002	0.361
DMSO	0.000	0.053
ethyl acetate	0.036	8.218
Toluene	0.014	3.146
Chloroform	0.089	20.515
1,4 dioxane	0.040	9.223
ethylene glycol	0.000	0.000
phenol	0.000	0.041
trifluoroethanol	0.036	8.329
2-butanone	0.036	8.224
methylene chloride (dichloromethane)	0.119	27.362
di(ethyl) ether	0.222	51.065
dimethyl ether	0.621	142.750
Methyl t-Butyl ether (MTBE)	0.126	29.048
triethylamine	0.028	6.505
tetrahydrofuran (THF)	0.066	15.229
Acetone	0.103	23.683

Table S2. Dimensions of the evaporation channels in the EL

		Evaporation channel layer dimensions (K'=6)				
		Length (cm)	Width (μm)	Height (μm)	Area of cross-section (A_C) (μm^2)	A_C/L (μm)
Rate of solvent evaporation (nL/hr)	3.75	2.7	150	100	15000	0.6
	7.5	1.8	220	100	22000	~1.2
	15	1.8	440	100	44000	~2.4
		Evaporation channel layer dimensions (K'=15)				
		Length (cm)	Width (μm)	Height (μm)	Area of cross-section (A_C) (μm^2)	A_C/L (μm)
Rate of solvent evaporation (nL/hr)	2	2.7	22.5/45/90	100/50/25	2250	0.084
	10	1.8	75/150/300	100/50/25	7500	~0.42
	50	1.8	378/750/1500	100/50/25	37500	~2.10
		Evaporation channel layer dimensions (K'=30)				
		Length (cm)	Width (μm)	Height (μm)	Area of cross-section (A_C) (μm^2)	A_C/L (μm)

Rate of solvent evaporation (nL/hr)	2	2.7	11.34/22.5/45	100/50/25	1134	0.042
	10	1.8	37.5/75/150	100/50/25	3750	~0.21
	50	1.8	189/378/750	100/50/25	18900	~1.05

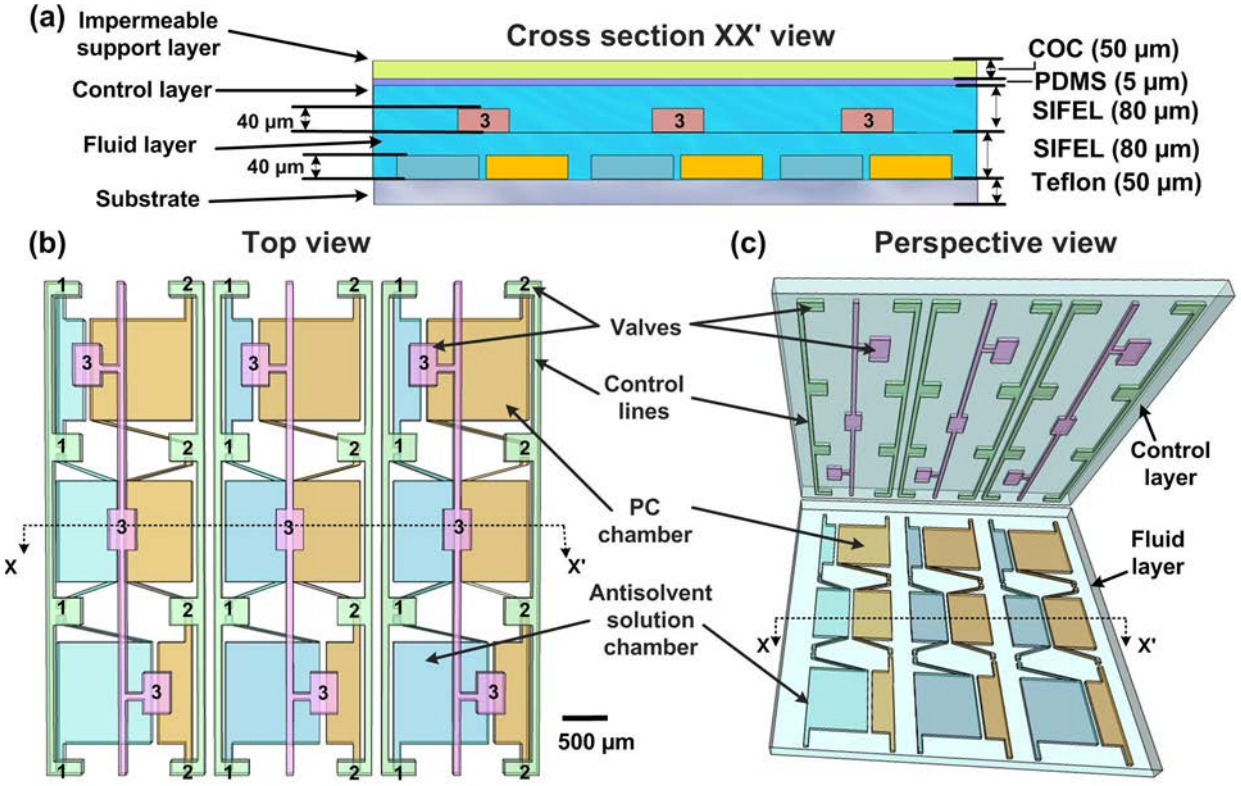

Figure S2. (a) Cross sectional view of three microfluidic crystallization wells showing the layered assembly of the platform. The platform comprises of the PDMS fluid and control layers sandwiched between layers of cyclic olefin copolymer (COC) on top and bottom to minimize solvent loss, to provide rigidity, and to enable Raman compatibility. The numbers 1, 2, and 3 refer to different sets of control valves. **(b)** Top view and **(c)** perspective view of a 3x3 array of microfluidic crystallization wells of the 72-well multiplexed platform depicting adjacent PC chamber (or PC/CCF chamber) and microseed solution chambers in the fluid layer, and pneumatic control lines and valves in the control layer. The top view illustrates the function of the different sets of valves (1, 2, 3) for filling and mixing of solutions.

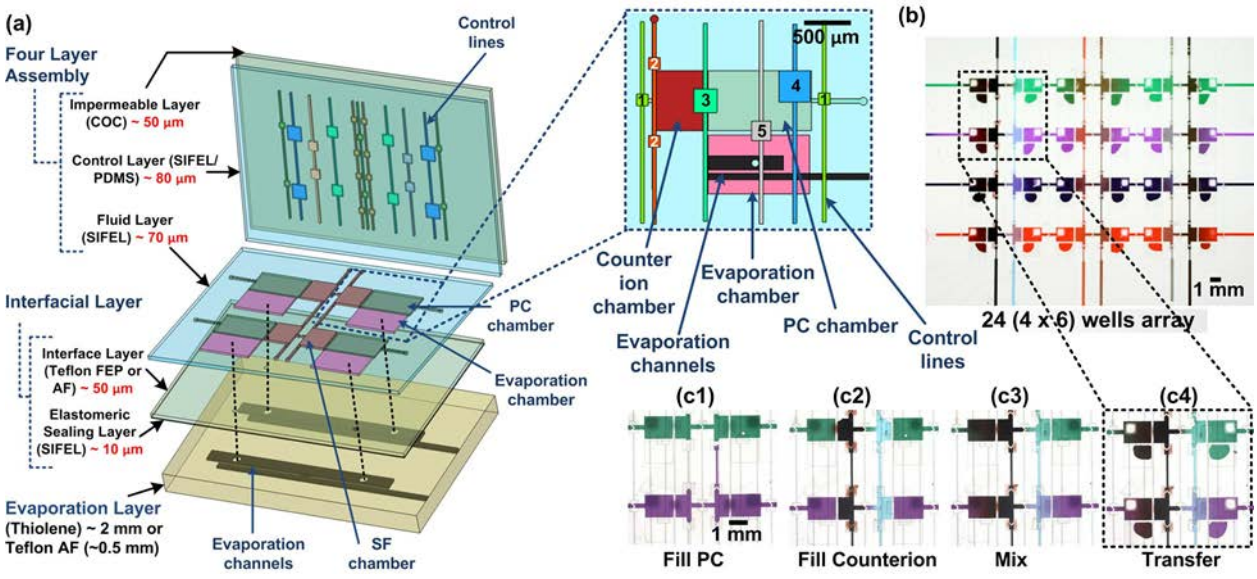

Figure S3. (a) Schematics of the layered design of a 2 x 2 array of wells in a microfluidic crystallization chip. The top section, referred to as the *Four Layer Assembly* comprised of an *Impermeable Layer* that minimizes solvent loss and provides rigidity, a *Control Layer* with pneumatic control lines and valves to enable fluidic routing and mixing, and a *Fluid Layer* with three chambers per well: two for PC and SF solutions and one that allows for solvent evaporation after mixing. An *Interfacial Layer* which ensures reversible sealing and allows for compatibility with Raman spectroscopy, connects the *Four Layer Assembly* with the bottom section, the *Evaporation Layer*, which contains the channels that allow solvent to evaporate at a certain rate. **(b)** Optical micrograph of the evaporation based microfluidic crystallization screening chip comprised of a 4 x 6 well array, filled with dyed solutions to highlight the chip's combinatorial mixing capabilities. **(c1-4)** Enlarged views of a 2 x 2 array of wells to visualize chip operation: PC solutions are introduced horizontally (valves 1 and 3 actuated) and locked up in the PC and SF chambers **(c1)**. SF solutions are introduced vertically (valves 2 actuated) and locked up in their respective chambers after the PC solutions are purged from these SF chambers by applying vacuum at the outlets **(c2)**. Adjacent PC and SF solutions are mixing (valves 3 actuated) **(c3)**. Back-and-forth movement of solutions (repeated actuation of valves 4) can be used to speed up the mixing process. The mixed solutions are then allowed to concentrate via solvent evaporation through the microchannels in the Evaporation Layer (valves 5 actuated) **(c4)**.

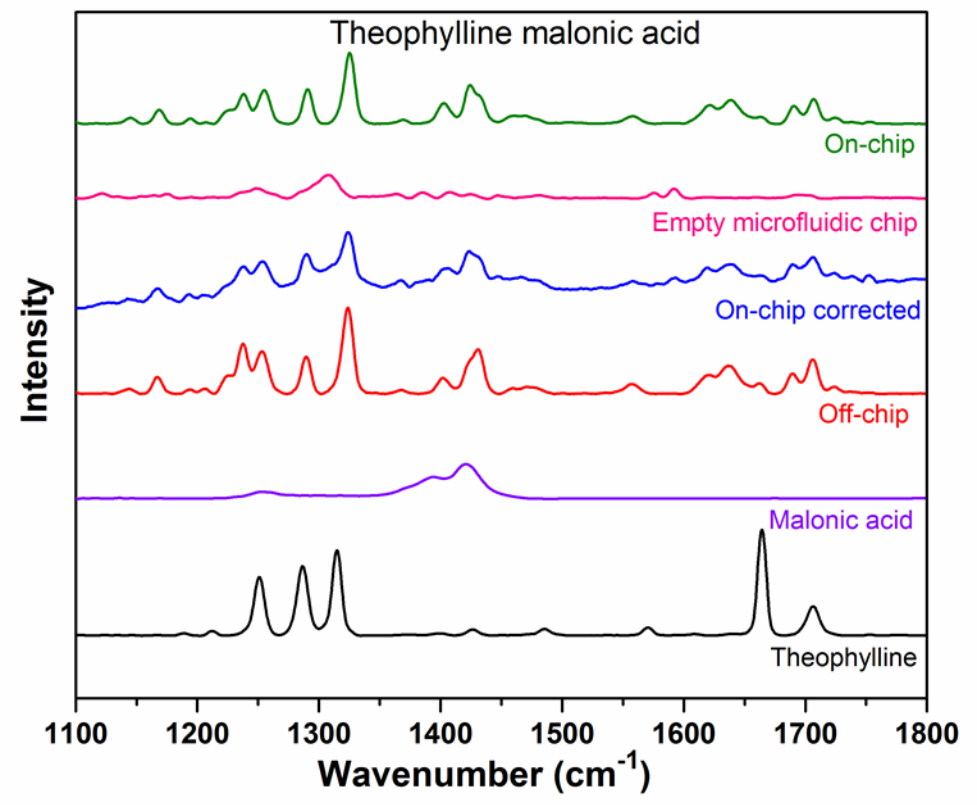

Figure S4

Raman spectra of theophylline and malonic acid as well as a theophylline malonic acid cocrystal grown and analyzed on-chip and off-chip. The views of the 1100-1800 cm^{-1} range are provided to highlight the lack or presence of spectral differences between the different cocrystals and/or samples grown on-chip and off-chip. "Empty microfluidic chip" corresponds to the Raman spectrum of the FLA-IL assembly by itself.

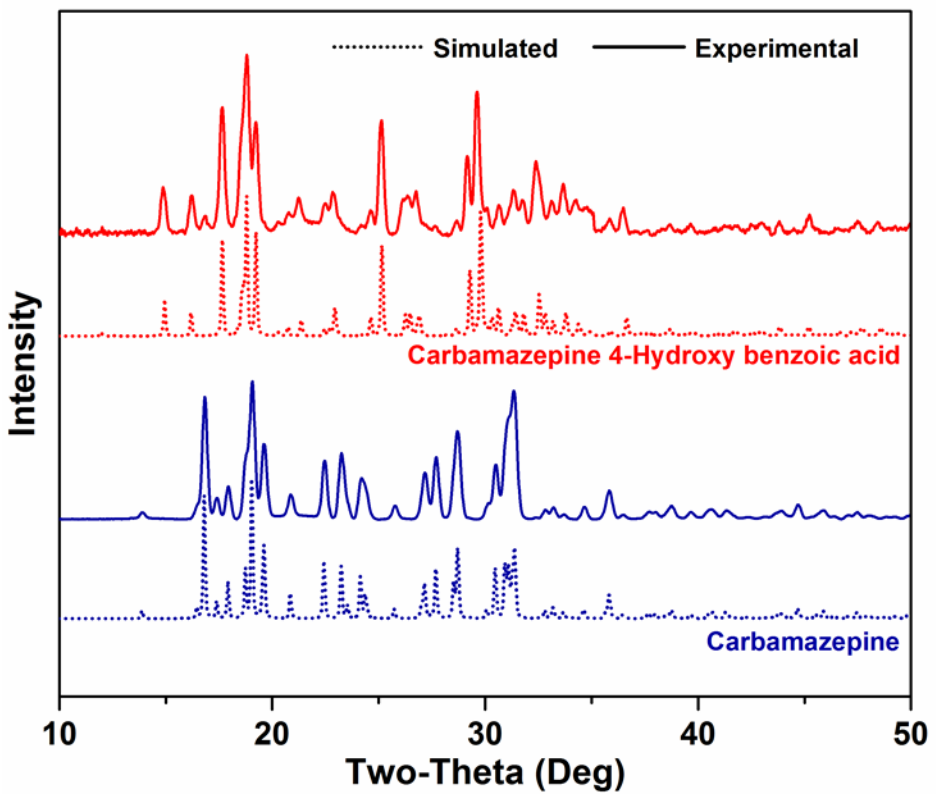

Figure S5

Powder diffraction data of carbamazepine and carbamazepine 4-hydroxybenzoic acid comparing experimental results (solid line) from solids grown on-chip and simulated data (dotted line) from crystal structures reported in the Cambridge Structural Database.